In Situ ATR-IR Spectroscopic and Reaction Kinetics Studies of Water−Gas Shift and Methanol Reforming on Pt/Al_2O_3 Catalysts in Vapor and Liquid Phases

Rong He, Rupali R. Davda, and James A. Dumesic*

Department of Chemical and Biological Engineering, University of Wisconsin−Madison, Madison, Wisconsin 53706

Received: October 5, 2004; In Final Form: November 22, 2004

Reaction kinetics measurements of the water−gas shift reaction were carried out at 373 K on Pt/Al_2O_3 in vapor phase to investigate the effects of CO, H_2, and H_2O partial pressures. Results of in situ ATR-IR studies conducted in vapor phase under similar conditions suggest that the Pt surface coverage by adsorbed CO is high (∼90% of the saturation coverage), leading to a negligible effect of the CO pressures on the rate of reaction. The negative reaction order with respect to the H_2 pressure is caused by the increased coverage of adsorbed H atoms, and the fractional positive order with respect to the water pressure is consistent with non-equilibrated H_2O dissociation on Pt. Results of in situ ATR-IR studies carried out at 373 K show that the presence of liquid water leads to a slight decrease in the Pt surface coverage by adsorbed CO (∼80% of the saturation coverage) when the CO partial pressure is the same as in the vapor-phase studies. The rate of the WGS reaction in the presence of liquid water is comparable to the rate under complete vaporization conditions when other factors (such as CO partial pressure) are held constant. Reaction kinetics measurements of methanol reforming were carried out at 423 K over a total pressure range of 1.36−5.84 bar. In situ ATR-IR studies were conducted at 423 K to determine the Pt surface coverage by adsorbed CO in completely vaporized methanol feeds and in aqueous methanol solutions. The decomposition of methanol is found to be slower during the reforming of methanol in liquid phase than in vapor phase, which leads to a lower rate of hydrogen production in liquid phase (0.08 min^{-1} at 4.88 bar) than in vapor phase (0.23 min^{-1} at 4.46 bar). The lower reaction order with respect to methanol concentration observed for vapor-phase versus liquid-phase methanol reforming (0.2 versus 0.8, respectively) is due to the higher extent of CO poisoning on Pt for reforming in vapor phase than in liquid phase, based on the higher coverage by adsorbed CO observed in completely vaporized methanol feeds (55−60% of the saturation coverage) than in aqueous methanol feed solutions (29−40% of the saturation coverage).

Introduction

The production of hydrogen for fuel cells and other industrial applications from renewable biomass-derived resources is a major challenge as global energy generation moves toward a "hydrogen society". We recently described a catalytic process for production of H_2 from aqueous solutions of biomass-derived oxygenated compounds such as methanol, ethylene glycol, glycerol, sugars, and sugar alcohols.[1−3] This process takes place over supported Pt catalysts at relatively low temperatures (e.g., 500 K) in the liquid phase, which eliminates the need to vaporize water and the oxygenated hydrocarbon, and produces hydrogen with low levels of CO (<300 ppm).[3,4] Reaction kinetics studies carried out for the aqueous-phase reforming of methanol and ethylene glycol suggest that the reforming may take place via CO as an intermediate product, which is subsequently converted to CO_2 by the water−gas shift (WGS) reaction. In this respect, monitoring the surface of Pt/Al_2O_3 catalysts in liquid phase under conditions similar to reaction kinetics studies should provide insight into the surface chemistry of this catalytic process.

In situ spectroscopic studies in the liquid phase are difficult due to interference from the bulk liquid. In this respect, spectroscopic studies of catalytic solid−liquid interfaces have been conducted using attenuated total reflectance infrared (ATR-IR) spectroscopy. Previously, in situ ATR-IR was used to study adsorption of oxygenated compounds (ethyl acetate, carboxylic acid) on oxide thin films grown on the ATR crystal using sol−gel methods.[5−8] Catalytic solid−liquid interfaces involving noble metals have also been studied using in situ ATR-IR. Zippel et al. investigated the adsorption of CO on Pt and Pd films (of 5 nm thick) from dry and wet gases and from liquid water with ATR-IR.[9] Recently, Baiker and co-workers studied the adsorption of CO from CH_2Cl_2 solvent on thin films of Pt (1 nm) and Pt/Al_2O_3 (1 nm Pt on top of 100 nm of Al_2O_3) coated on a Ge crystal.[10] The reaction of CO_2 with hydrogen in cyclohexane to form CO on the same Pt/Al_2O_3 model catalyst was followed by in situ ATR-IR spectroscopy at 313 K.[11] In another study, the adsorption of CO, pyridine, quinoline, 2-methylquinoline, and cinchonidine on Pd/Al_2O_3 and Pt/Al_2O_3 model catalysts was studied at 283 K in CH_2Cl_2 solvent.[12] In situ ATR-IR has also been extended to study supported noble metal catalyst in powder form. Burgi et al. studied enantioselective hydrogenation of a pyrone over a 5 wt % Pd/TiO_2 catalyst using ATR-IR measurements combined with phase-sensitive detection.[13] The adsorption of CO, formaldehyde, ethanol, and butyronitrile on a 5 wt % Pt/Al_2O_3 catalyst was studied in various solvents including water, ethanol, and hexane.[14] To our knowledge, the above in-

* To whom correspondence should be addressed. Fax: (608) 262-5434. E-mail: dumesic@engr.wisc.edu.

10.1021/jp045470k CCC: $30.25
Published on Web 01/26/2005

situ ATR-IR studies were carried out at near room temperature (<313 K) and ambient pressure. In the present study, we have extended in situ ATR-IR studies of catalytic solid−liquid interfaces to the elevated temperature of 423 K and a pressure of 5.84 bar for studying the aqueous-phase reforming reaction under conditions similar to reaction kinetics studies.

Reaction kinetics studies have been carried out previously in our group for the aqueous-phase reforming of methanol and ethylene glycol to investigate the effect of feed concentration and system pressure on the reaction rate.[4] These studies showed that the rate of ethylene glycol reforming was similar to the rate of methanol reforming, suggesting that the C−C cleavage step involved in reforming of ethylene glycol is not rate-limiting. Therefore, methanol reforming can serve as a model reaction for the reforming of oxygenated hydrocarbons with the general formula $C_nH_{2n+2}O_n$.

The decomposition of methanol on Pt has been studied under UHV conditions by HREELS and TPD.[15−17] On a clean Pt(111) surface, methanol decomposes at temperatures above 140 K to form adsorbed CO and H.[15] In another study, the decomposition of methanol on Pt(111) is observed at temperature between 180 and 200 K and is found to be controlled by the presence of defect sites, because only 1−2% of a monolayer of CO was formed regardless of the initial methanol coverage.[16] Recently, theoretical studies were carried out for methanol decomposition on Pt(111).[18−20] The pathway involving initial C−H activation is found to be more favorable energetically than the pathway involving initial O−H activation.

The above studies were conducted in the absence of liquid water. The electrooxidation of methanol on Pt electrodes in electrolyte solutions has been extensively studied using in situ infrared spectroscopy due to the potential of direct methanol fuel cells (DMFC).[21,22] In situ infrared spectroscopic studies of methanol electrooxidation have been carried out on polycrystalline Pt,[23−27] single-crystal Pt,[28,29] and Pt supported on glassy carbon.[30−32] In general, these studies identified adsorbed CO as the predominant species on Pt electrodes. The CO coverage on a 20% Pt/C electrocatalyst (with an average Pt particle size of 2.5 nm) was found to be 0.4−0.5 of saturation coverage in 0.1 M methanol at 0 V, based on comparison made between CO bands formed via methanol dissociation and by direct adsorption from solutions saturated with CO.[32] Jusys et al. observed that dehydrogenation of methanol was inhibited as the CO coverage in 0.1 M methanol reaches about half of the saturation coverage on a similar 20% Pt/C electrocatalyst.[33] Park et al. observed that the extent of CO formation on Pt diminished with decreasing Pt particle size on various Pt/C samples with average Pt particle sizes ranging from 8.8 to 2.0 nm.[34]

In the first part of this paper, we focus on the WGS reaction on Pt catalysts in vapor phase and in the presence of liquid water at 373 K. In situ ATR-IR studies are conducted to investigate the effects of CO and H_2 in vapor phase on the reaction kinetics measured under similar conditions, and these results are compared with spectra from in situ ATR-IR studies conducted for the WGS reaction in the presence of liquid water to probe the effects caused by liquid water. In the second part of the paper, we study the reforming of methanol at 423 K in vapor phase and liquid phase using in situ ATR-IR spectroscopy and reaction kinetics measurements to obtain an understanding of the differences between methanol reforming in vapor-phase and in liquid-phase reaction conditions.

Experimental Section

Reaction Kinetics. Reaction kinetics data were collected using an alumina-supported catalyst (γ-Al_2O_3 extrudate, Topsøe) prepared via ion-exchange.[35,36] The alumina support (150 m^2/g) was placed in contact with an aqueous solution of tetraamine platinum nitrate ($Pt(NH_3)_4(NO_3)_2$, Strem Chemicals) for 24 h on a rotary shaker with an oxide surface area per liter of solution of 500 m^2/L. The pH value of the aqueous solution was adjusted to 11.5 using NaOH prior to the addition of the alumina support. The ion-exchanged sample was dried in an oven at 373 K for 24 h and was subsequently heated to 533 K (1.3 K/min) in a mixture of 10% O_2/He (300 cm^3(STP)/min) in a Pyrex cell and held at 533 K for 2 h. The Pt loading on the catalyst was 0.9 wt % as determined by atomic absorption spectroscopy of the calcined samples (AAS/ICP).

Prior to collection of reaction kinetics data, the calcined catalyst was reduced on the kinetics apparatus in H_2 (100 cm^3(STP)/min). The reactor was heated to 533 K (1.3 K/min) and held at this temperature for 2 h. Carbon monoxide chemisorption at 300 K was performed as described elsewhere[2] on the calcined catalyst after an identical treatment, and the number of catalytic sites was taken to be the irreversible CO uptake (i.e., 30 μmol/g).

The apparatus used to conduct reaction kinetics studies of the WGS reaction (vapor phase) and methanol reforming (vapor and liquid phase) is described in detail elsewhere.[4] Briefly, liquid feed is introduced in an up-flow configuration into the reactor, and the effluent is cooled with cooling water before entering the gas−liquid separator. For reaction kinetics studies of the WGS reaction in vapor phase, CO mixtures balanced with N_2 and/or H_2, together with deionized water (introduced at 0.01−0.06 mL/min with a syringe pump), were preheated before being introduced into a 25.4-mm o.d. (1 in.) and 23-mm i.d. Pyrex tubular reactor containing 0.5 g of catalyst. The total system pressure was regulated from 1.01 to 1.63 bar. The CO concentration of the effluent gas stream was obtained using a Siemens Ultramat 5E gas analyzer.

Reaction kinetics studies of the vapor- and liquid-phase reforming of methanol were conducted using solutions of 2 or 5 wt % methanol in deionized water. These solutions were fed at 0.05 mL/min with an HPLC pump to a 12.7-mm o.d. ($^1/_2$ in.) and 11.3-mm i.d. stainless steel tubular reactor containing 4.5 g of catalyst. The total pressure of the system was regulated from 1.36 to 5.84 bar with N_2 carrier gas, which bubbled through the effluent and swept the gaseous products for analysis to gas chromatographs. The results of replicate measurements agreed to within ±5%.

In Situ ATR-IR Spectroscopy. In situ ATR-IR studies of the WGS reaction and methanol reforming were carried out using a 2.1 wt % Pt/Al_2O_3 catalyst prepared by multiple incipient wetness impregnation of fine alumina powder (γ-Al_2O_3, Alfa Aesar, mean particle size 3 μm) with an aqueous solution of tetraamine platinum nitrate ($Pt(NH_3)_4(NO_3)_2$, Strem Chemicals). The impregnated sample was calcined and characterized in ways identical to that of the sample used for reaction kinetics studies. The Pt loading on this catalyst was determined with AAS/ICP, and the amount of irreversible CO uptake at 300 K on this catalyst is 61 μmol/g.

The calcined catalyst powder was deposited onto the ATR crystal (ZnSe, 45°, 80 × 10 × 3 mm, Thermo Electron) using a suspension of the catalyst (20 mg) in 4 mL of deionized water that had been placed in an ultrasonic bath for 8−12 h (to obtain a uniform suspension). The suspension was spread onto one side of the ZnSe crystal and dried under ambient conditions for at least 12 h before use. The amount of suspension used was 0.6 mL in the experiments conducted in vapor phase, and it was 0.2 mL (diluted into 0.4 mL deionized water) for the

TABLE 1: Operating Conditions and Results of Reaction Kinetics Studies of the Water−Gas Shift Reaction in Vapor Phase

	condition no.							
	1	2	3	4	5	6	7	8
system pressure (bar)	1.65	1.68	1.67	1.64	1.64	1.03	1.25	1.65
dry gas CO concentration (ppm)	277	574	990	1000	1005	1005	1005	1005
dry gas flow rate (cm^3/min)	69.6	71.5	68.7	68.1	69.6	70.6	71.0	72.6
water feed (mL/min)	0.02	0.02	0.02	0.02	0.02	0.01	0.03	0.06
CO partial pressure (mbar)	0.34	0.97	1.17	1.22	1.21	0.88	0.82	0.82
H_2O partial pressure (bar)	0.44	0.44	0.42	0.41	0.43	0.15	0.43	0.83
H_2 partial pressure (bar)	1.21	1.24	1.25	0.54	1.9×10^{-4}	0.8×10^{-4}	1.0×10^{-4}	1.8×10^{-4}
N_2 partial pressure (bar)	0.00	0.00	0.00	0.68	1.21	0.88	0.82	0.81
conversion (%)	5.7	9.3	3.6	6.0	16.0	8.7	12.3	22.3
TOF (min^{-1})	0.0086	0.0076	0.0081	0.0128	0.0343	0.0189	0.0270	0.0496

experiments conducted in liquid phase to ensure a good seal made by the O-ring. The film thickness is estimated to be ~5 μm based on the density of alumina when 0.6 mL of suspension was used, and the alumina support used for this catalyst has an average particle size of 3 μm. The evanescent wave generated at the interface (with a penetration depth of ~1 μm) thus probes part of the catalyst film, along with the interstitial solution.

ATR-IR spectra were recorded using a horizontal flow cell (Thermo Electron), in which the coated ATR crystal was sealed with a viton O-ring to a Teflon-coated aluminum frame. The length and width of the oval-shaped exposed area are 70 × 8 mm, respectively. The total volume of the flow cell is ~65 μL. The flow cell was heated to 423 K with heating cartridges integrated in the aluminum frame and pressurized to 5.84 bar. The cell was mounted onto an ATR accessory (Thermo Electron) within the FTIR spectrometer (Matteson Galaxy 3020). The cell was connected to an apparatus similar to the reaction kinetics apparatus. Liquid feed was introduced into the cell with an HPLC pump. Prior to entering the flow cell, the reactant stream was preheated to the same temperature as the flow cell by flowing through a heated titanium tube (3.2-mm o.d. ($^1/_8$ in.), 0.61-m long).

In situ ATR-IR studies of the WGS reaction in vapor phase were carried out at 373 K and 1.63 bar. A reference spectrum was first collected on the dry catalyst layer at 303 K in He (70 cm^3 (STP)/min). The catalyst layer was then heated to 373 K (1.75 K/min) in He with deionized water flowing at 0.02 mL/min (leading to 0.4 bar H_2O in vapor phase), and another reference spectrum was collected. The calcined catalyst layer was subsequently exposed to (and reduced by) 333 ppm CO/H_2 (dry basis, 70 cm^3 (STP)/min) with 0.4 bar H_2O in vapor phase for 1.5 h, and a spectrum was taken. The CO concentration in H_2 was increased to 1000 ppm, and another spectrum was collected. The flow of deionized water was then stopped, and another spectrum was taken over the drying period of 0.5 h. The catalyst layer was subsequently cooled to 303 K in 1000 ppm CO/H_2, and a final spectrum was collected. In another experiment, the catalyst layer was first exposed to 333 ppm CO/H_2, and then exposed to 333 and 1000 ppm CO/He sequentially, all in the presence of 0.4 bar H_2O vapor. Each gas mixture was given 1.5 h to reach steady state, and a spectrum was taken at the end of each period. The catalyst layer was then dried and cooled to 303 K in 1000 ppm CO/He, and two more spectra were taken at 373 and 303 K, respectively.

In situ ATR-IR studies of the WGS reaction in the presence of liquid water were carried out at 373 K and 2.22 bar (to keep the partial pressures of dry gases the same as in the vapor-phase studies conducted at 1.63 bar). The flow rate of deionized water was maintained at 0.10 mL/min throughout the experiments, and the gas flow rate was 70 cm^3 (STP)/min. A reference spectrum was collected of the calcined catalyst layer in liquid water at 303 K with flowing He. The catalyst layer was then heated to 373 K (1.75 K/min) in liquid water with flowing He, and another reference spectrum was collected. The catalyst layer in liquid water was exposed to 333 and 1000 ppm CO/H_2 sequentially for 6 and 1.5 h, respectively, and a spectrum was taken at the end of each period. The catalyst layer was then cooled to 303 K in 1000 ppm CO/H_2, and a final spectrum was taken in the presence of liquid water. In another experiment, the catalyst layer in liquid water was first exposed to 333 ppm CO/H_2 for 6 h, and then exposed to 333 and 1000 ppm CO/He sequentially (both for 1.5 h), with a spectrum taken at the end of each period. The catalyst layer was subsequently cooled to 303 K in 1000 ppm CO/He, and a final spectrum was taken in the presence of liquid water.

In situ ATR-IR studies of the vapor-phase reforming of methanol were carried out at 423 K and at the pressure of 1.36 or 3.08 bar. A reference spectrum was first collected of the dry catalyst layer at 303 K in He (50 cm^3 (STP)/min). The catalyst layer was then heated to 423 K (2 K/min) in He. The He gas flow into the ATR-IR flow cell was stopped, deionized water was introduced into the ATR-IR flow cell at 0.05 mL/min for 1 h, and a reference spectrum was collected. The catalyst layer was then dried in flowing He for 0.5 h and reduced in flowing H_2 for 0.5 h, both gases flowing at 50 cm^3 (STP)/min. The H_2 flow was stopped, aqueous methanol feed was introduced into the flow cell (where the feed was completely vaporized) at 0.05 mL/min for 1 h, and a spectrum was collected. The catalyst layer was then dried in flowing H_2 for 0.5 h at 423 K, and cooled to 303 K (2 K/min). A final spectrum was collected at 303 K after the H_2 was replaced with 1000 ppm CO/H_2 for 0.5 h.

In situ ATR-IR studies of the liquid-phase reforming of methanol were carried out at 423 K and 5.84 bar. A reference spectrum was first collected of the calcined catalyst layer at 303 K with He flowing at 50 cm^3 (STP)/min and deionized water flowing at 0.1 mL/min. The catalyst layer was then heated to 423 K (2 K/min) with He flowing at 3 cm^3 (STP)/min and deionized water flowing at 0.2 mL/min, and another reference spectrum was collected. The catalyst layer was subsequently dried in flowing He for 0.5 h and reduced in flowing H_2 for 0.5 h, both gases flowing at 50 cm^3 (STP)/min. The H_2 flow was then reduced to 3 cm^3 (STP)/min, 2 or 5 wt % methanol in deionized water was introduced into the flow cell at 0.2 mL/min, and three spectra were collected sequentially over a period of 1 h. The catalyst layer was then dried briefly (<1 min) in H_2 flowing at 50 cm^3 (STP)/min, followed by cooling to 303 K (2 K/min). The dry catalyst layer was exposed to 1000 ppm CO/H_2 flowing at 50 cm^3 (STP)/min for 1 h, deionized water was then introduced into the flow cell at 0.1 mL/min, and a final spectrum was taken.

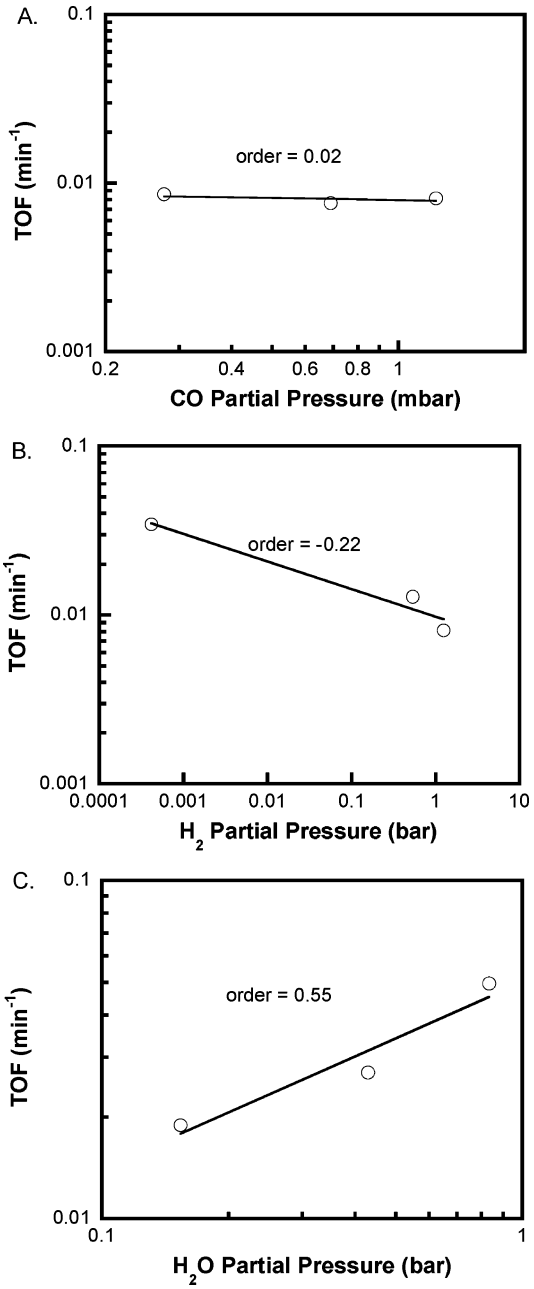

Figure 1. (A) The effect of CO partial pressure on the rate of WGS reaction over the range of 0.34−1.17 mbar at 373 K and a total pressure of 1.6 bar; (B) the effect of H_2 partial pressure on the rate of WGS reaction over the range of 1.9×10^{-4} to 1.25 bar at 373 K and a total pressure of 1.6 bar; and (C) the effect of H_2O partial pressure on the rate of WGS reaction over the range of 0.15−0.83 bar at 373 K and a total pressure range of 1.0−1.6 bar.

All infrared spectra were collected in the absorbance mode using 1024 scans with a resolution of 4 cm^{-1}. Spectra reported in the present study are spectra of the catalyst under controlled conditions minus the IR spectrum of the calcined sample hydrated similarly at the same temperature and pressure.

Results

Reaction Kinetics Studies of WGS Reaction. Table 1 summarizes the operating conditions and results of reaction kinetics measurements of the WGS reaction in the vapor phase. The partial pressures of gases are calculated on the basis of the water feed rate, gas composition, and gas flow rate. Figure 1A shows the rate of WGS reaction versus the CO partial pressure

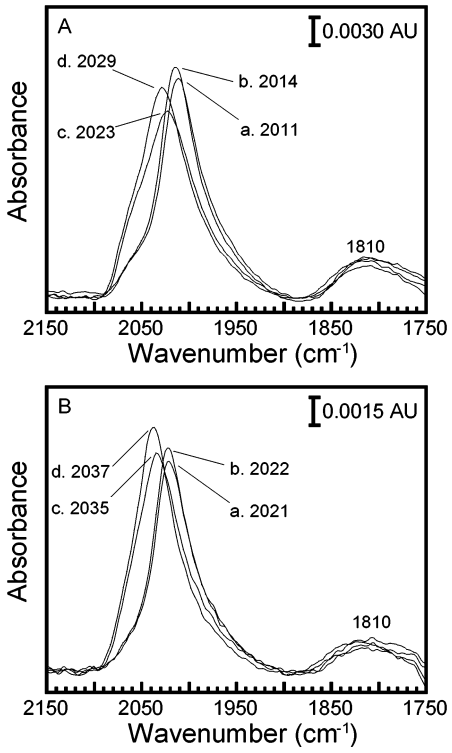

Figure 2. (A) ATR-IR spectra of CO adsorbed on Pt/Al_2O_3 catalyst exposed to (a) 333 ppm CO/H_2 (dry basis) with 0.4 bar H_2O at 373 K, (b) 1000 ppm CO/H_2 (dry basis) with 0.4 bar H_2O at 373 K, (c) 1000 ppm CO/H_2 (dry basis) after the water feed was stopped at 373 K, and (d) 1000 ppm CO/H_2 (dry basis) after the sample was subsequently cooled to 303 K; (B) ATR-IR spectra of CO adsorbed on Pt/Al_2O_3 collected under conditions similar to the spectra in (A), except that the gas mixtures are He-balanced instead of H_2-balanced.

in the presence of 1.2 bar of H_2 and 0.4 bar of H_2O (corresponding to columns 1−3 in Table 1). The reaction order with respect to CO partial pressure is 0.02 between 0.34 and 1.17 mbar of CO. Figure 1B shows the rate of the WGS reaction versus the H_2 partial pressure in 1.2 mbar of CO and 0.4 bar of H_2O (corresponding to column 3−5 in Table 1). The reaction order with respect to H_2 partial pressure is −0.22 between 1.9×10^{-4} and 1.25 bar of H_2. The effect of H_2O partial pressure in the presence of 0.82−0.88 mbar of CO is shown in Figure 1C (corresponding to columns 6−8 in Table 1). The reaction order with respect to H_2O partial pressure is 0.55 between 0.15 and 0.83 bar of H_2O. Previous studies by Genoble et al. reported that the order with respect to CO is −0.21 and the order with respect to H_2O is 0.74 on a Pt/Al_2O_3 catalyst at 543 K.[37] Lam et al. found a reaction order of 0.45 with respect to CO, 0.37 with respect to H_2O, and −0.23 with respect to H_2 on Pt/Al_2O_3 at a much higher temperature of 817 K.[38]

In Situ ATR-IR Studies of WGS Reaction. Results of in-situ ATR-IR studies of the WGS reaction in vapor phase at 373 K and 1.63 bar are shown in Figure 2. Spectra a and b in Figure 2A were collected while the Pt/Al_2O_3 catalyst was exposed to 333 and 1000 ppm CO/H_2 sequentially with 0.4 bar H_2O vapor at 373 K. A band at 2011 cm^{-1} and another broad band at ∼1810 cm^{-1} were observed in spectrum a, which can be assigned to linear-bonded (L) CO and bridge-bonded (B) CO, respectively. The frequency of 2011 cm^{-1} for the CO(L) band is lower than the normal range of 2040−2070 cm^{-1} observed for CO adsorption on Pt/Al_2O_3. We have observed CO(L) bands at 2044 and 2057 cm^{-1} on this catalyst in 10% CO in H_2 and He, respectively, at 373 K without H_2O vapor, which can be assigned to CO adsorbed on Pt sites with low

coordination numbers.[39−41] The Pt dispersion of this catalyst reduced at 533 K is approximately 80% based on CO chemisorption results, which indicates that the average size of the Pt particle is ∼1.5 nm, assuming the surface of the Pt particles consists of equal percentages of (111), (110), and (100) surfaces. Therefore, the stretching frequency of 2057 cm^{-1} observed in 10% CO/He is consistent with the small Pt particle size. The slightly lower frequency of 2044 cm^{-1} observed in 10% CO/H_2 can be attributed to coadsorption of H_2, because previous studies have shown that coadsorption of H_2 with CO on Pt leads to a small decrease of CO stretching frequency by 5−10 cm^{-1}.[42,43] Importantly, several studies have shown that coadsorption of H_2O with CO leads to a decrease in frequency of linear-bonded CO. In particular, Bourane et al. observed a shift of the CO stretching frequency from 2075 cm^{-1} in 1% CO/He to 2045 cm^{-1} in 1% CO/3.5% H_2O/He on Pt/Al_2O_3 at 300 K.[44] A shift of the CO(L) band from 2065 to 2050 cm^{-1} was observed on Pt/Al_2O_3 with the introduction of an excess of H_2O vapor.[45] On a thin Pt layer, the presence of H_2O vapor led to a shift of the CO(L) band from 2060 to 2030 cm^{-1}.[9] Therefore, on the basis of these previous studies, we attribute the low frequency of 2011 cm^{-1} observed to the adsorption of CO in the presence of H_2O vapor and H_2.

The CO(L) band in Figure 2A shifted to 2014 cm^{-1} and increased slightly in intensity as the CO concentration in H_2 was increased to 1000 ppm. The CO(L) band then shifted to 2023 cm^{-1} during the drying period of 0.5 h in 1000 ppm CO/H_2, and the integrated intensity of this band in spectrum c is essentially the same as in spectrum b, although the band has lower intensity and larger half-width. Bourane et al. reported similar changes in band shape, and they found that the extinction coefficient of linear-bonded CO species is not modified strongly in the presence of H_2O.[44] The intensity of the CO(L) band then increased slightly after the sample was cooled to 303 K in 1000 ppm CO/H_2 (spectrum d). The ratios of integrated intensities of the CO(L) bands in spectra a and b to that in spectrum d in Figure 2A are 0.94 and 0.97, respectively.

Spectra a and b in Figure 2B correspond to CO adsorbed on Pt/Al_2O_3 under conditions similar to spectra a and b in Figure 2A (with 0.4 bar H_2O vapor at 373 K), except that the 333 and 1000 ppm CO gas mixtures are balanced using He, instead of H_2. The CO(L) bands in spectra a and b were observed at 2021 and 2022 cm^{-1}, respectively, with similar intensity, as compared to the frequency of 2011 and 2014 cm^{-1} observed for the CO(L) bands in spectra a and b in Figure 2A (in H_2-balanced gas mixtures). Drying the Pt/Al_2O_3 catalyst in 1000 ppm CO/He for 0.5 h at 373 K leads to an increase in CO(L) band frequency to 2035 cm^{-1}, and a slight increase in integrated intensity of the CO(L) band. The intensity of the CO(L) band then increased slightly after the sample was cooled to 303 K in 1000 ppm CO/He (spectrum d). The ratios of integrated intensities of the CO(L) bands in spectra a and b to that in spectrum d in Figure 2B are 0.88 and 0.91, respectively.

Results of in situ ATR-IR studies of the WGS reaction at 373 K and 2.22 bar in the presence of liquid water are shown in Figure 3. A linear-bonded CO band was observed at 2007 cm^{-1} when the Pt/Al_2O_3 catalyst was exposed to 333 ppm CO/H_2 at 373 K in the presence of liquid water, as shown in spectrum a in Figure 3A. The intensity of the CO(L) band increased slightly as the CO concentration was increased from 333 to 1000 ppm, and the band shifted to 2011 cm^{-1} (spectrum b). The CO(L) band shifted to 2020 cm^{-1} and gained intensity as the Pt/Al_2O_3 catalyst was then cooled to 303 K in 1000 ppm CO/H_2 in liquid water (spectrum c). Previously, Ferri et al.

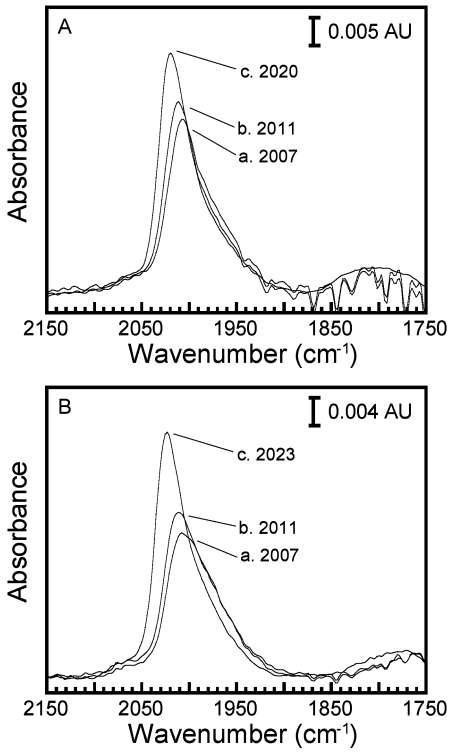

Figure 3. (A) ATR-IR spectra of CO adsorbed on Pt/Al_2O_3 as the catalyst in liquid water was exposed to (a) 333 ppm CO/H_2 (dry basis) at 373 K, (b) 1000 ppm CO/H_2 (dry basis) at 373 K, and (c) 1000 ppm CO/H_2 (dry basis) after the sample was cooled to 303 K; (B) ATR-IR spectra of CO adsorbed on Pt/Al_2O_3 collected under conditions similar to the spectra in (A), except that the gas mixtures are He-balanced instead of H_2-balanced.

observed a CO(L) band at 2058 cm^{-1} with a shoulder at 2000 cm^{-1} in ATR-IR spectra of CO collected on a model Pt/Al_2O_3 catalyst in liquid water at room temperature.[10] The adsorption of CO on a powdered Pt/Al_2O_3 catalyst in liquid water at room temperature led to a CO(L) band at 2052 cm^{-1} in ATR-IR spectra.[14] We attribute the lower frequency observed here to the presence of low-coordination Pt sites on our catalyst due to the low calcination and reduction temperature. The ratios of integrated intensities of the CO(L) bands in spectra a and b to that in spectrum c in Figure 3A are 0.80 and 0.84, respectively. The spectra in Figure 3B were collected under conditions similar to the spectra in Figure 3A, except that the 333 and 1000 ppm gas mixtures were balanced using He, instead of H_2. The ratios of integrated intensities of the CO(L) bands in spectra a and b to that in spectrum c in Figure 3B are 0.78 and 0.81, respectively.

We observed a considerable decrease in the intensity of the CO(L) band when the catalyst layer in 333 ppm CO/H_2 was subsequently exposed to 333 ppm CO/He in the presence of 0.4 bar H_2O, as shown in spectra a and b in Figure 4A, respectively. A similar decrease in the intensity of CO(L) band was observed when the catalyst layer in 333 ppm CO/H_2 was subsequently exposed to 333 ppm CO/He in the presence of liquid water, as shown in spectra a and b in Figure 4B, respectively. To interpret these results, another experiment was conducted using an in situ transmission IR flow cell with short path length (∼5 mm) under conditions identical to those in Figure 4A, and the CO(L) band intensity remained constant as the gas flow was switched from 333 ppm CO/H_2 to 333 ppm CO/He in the presence of 0.4 bar H_2O vapor. Therefore, the changes in intensity of CO(L) bands observed in Figure 4A and B are not due to changes in surface CO coverage. These artifacts

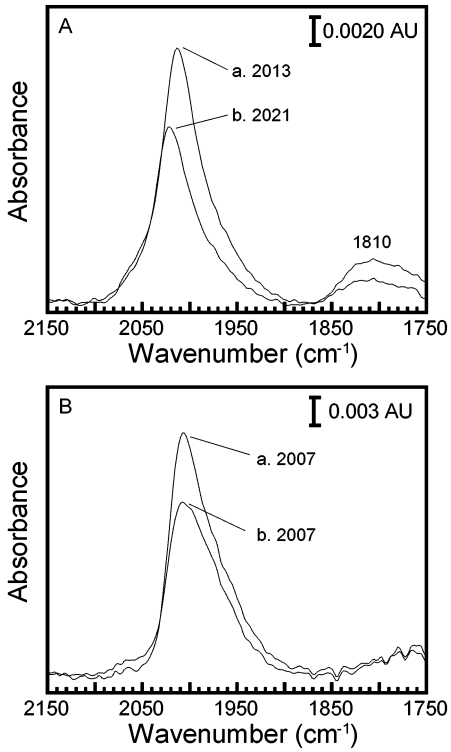

Figure 4. (A) ATR-IR spectra of CO adsorbed on Pt/Al_2O_3 catalyst exposed to (a) 333 ppm CO/H_2 (dry basis) and (b) 333 ppm CO/He (dry basis) with 0.4 bar H_2O in vapor phase at 373 K; (B) ATR-IR spectra of CO adsorbed on Pt/Al_2O_3 catalyst exposed to (a) 333 ppm CO/H_2 (dry basis) and (b) 333 ppm CO/He (dry basis) in the presence of liquid water at 373 K.

of ATR-IR were generally induced by a change in gas atmosphere at elevated temperatures and, importantly, in the presence of water, especially liquid water. To minimize these artifacts, the catalyst layers were saturated with CO by cooling to 303 K in the same 1000 ppm gas mixtures as at 373 K, instead of by increasing the CO concentration in the gas mixtures at 373 K.

Reaction Kinetics Studies of Methanol Reforming. Figure 5A shows the rates of hydrogen production from methanol reforming at 423 K versus the system pressure. The reaction order with respect to system pressure is 0.3 in vapor phase (up to 4.46 bar) using 2 or 5 wt % methanol feed. In contrast, the reaction order with respect to system pressure in liquid phase (above 4.88 bar) is highly negative (ca. −6 order) for 2 and 5 wt % methanol feeds. A similar inhibiting effect of system pressure on rate of hydrogen production has been observed for the liquid-phase reforming of methanol at 498 K and was mainly attributed to an increase in hydrogen partial pressure as the system pressure increases.[4] In short, the gaseous bubbles formed during the liquid-phase reforming of methanol are composed of the reaction products plus the water and methanol at their respective vapor pressures. The hydrogen partial pressure in the catalyst bed is then calculated assuming the total pressure of the bubbles is equal to the total pressure of the system. Figure 5B shows a plot of the rate of hydrogen production from liquid-phase methanol reforming versus the calculated hydrogen partial pressure. The reaction order with respect to the calculated hydrogen partial pressure is −0.7 for 2 and 5 wt % methanol feed. We also note that the rate of hydrogen production at 4.46 bar (vapor-phase reforming) is 0.23 min^{-1}, which is much higher than the rate of 0.08 min^{-1} observed at 4.88 bar (liquid-phase reforming).

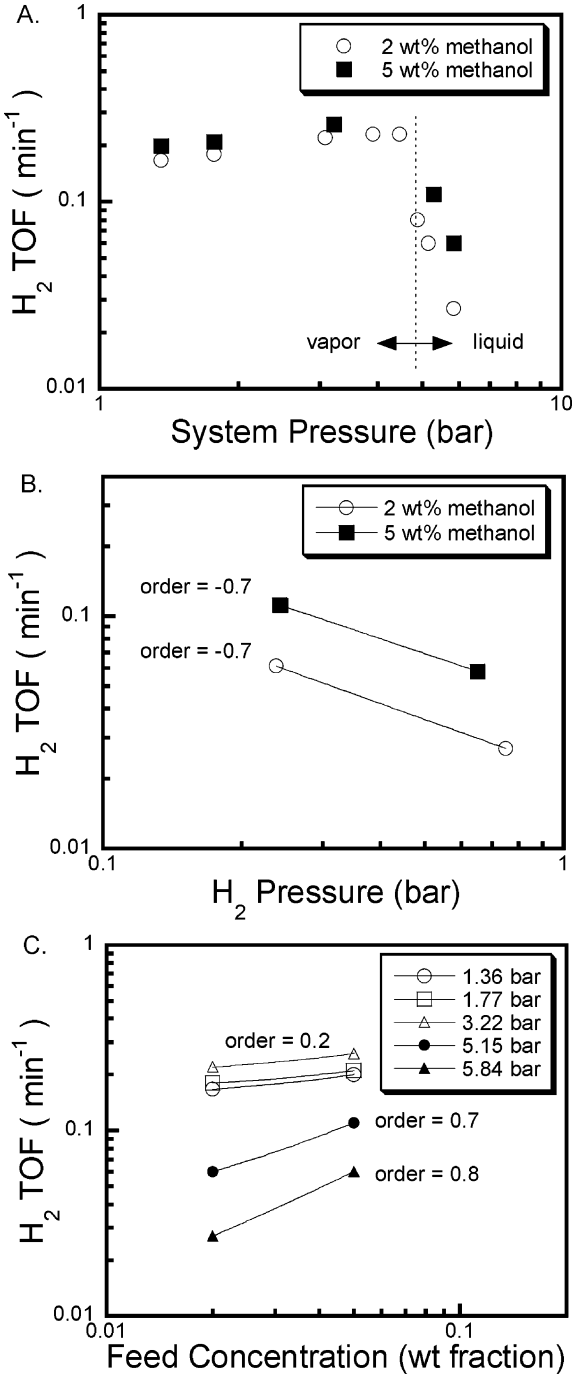

Figure 5. (A) The effect of total system pressure on the rate of hydrogen production from the vapor- and liquid-phase reforming of 2 and 5 wt % methanol at 423 K over a total pressure range of 1.36−5.84 bar; (B) the effect of hydrogen partial pressure on the rate of hydrogen production from the liquid-phase reforming of 2 and 5 wt % methanol feed at 423 K over a total pressure range of 4.88−5.84 bar; and (C) the effect of methanol concentration on the rate of hydrogen production from the vapor and liquid-phase reforming of methanol at 423 K over the range of 2−5 wt % at various system pressures.

Figure 5C shows the effect of feed concentration on the rate of hydrogen production at various system pressures. For vapor-phase reforming, the reaction order with respect to methanol feed concentration is 0.2 at 1.36, 1.77, and 3.22 bar. In contrast, for liquid-phase reforming, the reaction order with respect to feed concentration is 0.7 and 0.8 at 5.15 and 5.84 bar, respectively.

The results of reaction kinetics measurements of methanol reforming are summarized in Table 2. For the liquid-phase

TABLE 2: Operating Conditions and Results of Reaction Kinetics Studies of the Vapor- and Liquid-Phase Reforming of Methanol

				vapor-phase partial pressures				
feed (wt %)	system P (bar)	H_2 TOF (min^{-1})	conversion (%)	H_2	CO_2	CH_4O	H_2O	% vaporization of water
2	1.36	0.17	25.3	0.011	0.004	0.012	1.33	100
2	1.77	0.18	28.9	0.016	0.006	0.014	1.74	100
2	3.08	0.22	31.2	0.033	0.011	0.024	3.01	100
2	3.91	0.23	33.4	0.044	0.014	0.029	3.82	100
2	4.46	0.23	31.8	0.050	0.016	0.034	4.37	100
2	4.88	0.08	13.4	0.033	0.012	0.140	4.69	59
2	5.15	0.06	9.2	0.238	0.083	0.140	4.69	6
2	5.84	0.03	4.9	0.749	0.261	0.140	4.69	1
5	1.36	0.20	11.6	0.013	0.005	0.034	1.30	100
5	1.77	0.21	13.2	0.019	0.007	0.044	1.70	100
5	3.22	0.26	15.8	0.042	0.014	0.077	3.09	100
5	5.29	0.11	6.1	0.242	0.076	0.355	4.61	11
5	5.84	0.06	3.4	0.651	0.218	0.355	4.61	2

reforming of 2 wt % methanol feed at system pressures of 4.88, 5.15, and 5.84 bar, we calculate that 59%, 6%, and 1% of water in the feed was vaporized, respectively. For the liquid-phase reforming of 5 wt % methanol at system pressures of 5.29 and 5.84 bar, we calculate that 11% and 2% of water in the feed was vaporized, respectively.

In situ ATR-IR Studies of Methanol Reforming. Figure 6A shows ATR-IR spectra collected for the vapor-phase methanol reforming at 423 K and 1.36 bar. A band at 1986 cm^{-1} was observed when the catalyst layer was exposed to completely vaporized 2 wt % methanol feed (without co-feeding H_2) at 423 K (spectrum a) and is attributed to linear-bonded CO species formed on Pt via methanol decomposition. The CO band then shifted to ~2010 cm^{-1} and broadened (leading to higher integrated intensity) when the catalyst layer was dried and cooled to 303 K in flowing H_2 (spectrum not shown). The CO band subsequently shifted to 2032 cm^{-1} and gained more intensity after the catalyst layer was exposed to 1000 ppm CO/H_2 at 303 K subsequently (spectrum b). The ratio of integrated intensity of the CO(L) band in spectrum a to that in spectrum b is 0.55, which suggests that the surface CO coverage in completely vaporized 2 wt % methanol feed at 1.36 bar and 423 K is ~55% of the saturation coverage. The low frequency observed for the CO band in spectrum a (1986 cm^{-1}) is consistent with the estimated low coverage of CO and with the presence of 1.3 bar H_2O vapor.

Analogous experiments were conducted using 5 wt % methanol feed to examine the effect of methanol partial pressure, and the results are shown in Figure 6B. Exposing the catalyst layer to completely vaporized 5 wt % methanol feed (without co-feeding H_2) at 423 K leads to a linear-bonded CO band at 1988 cm^{-1} (spectrum a). The ratio of integrated intensity of the CO(L) band in spectrum a to that in spectrum b (collected for a CO-saturated catalyst at 303 K) is 0.60, as compared to the corresponding ratio of 0.55 obtained using 2 wt % methanol feed.

Figure 6C shows ATR-IR spectra collected for the vapor-phase methanol reforming at 3.08 bar using 0.9 wt % methanol feed. The methanol partial pressure in vapor phase is the same as in the experiment conducted at 1.36 bar using 2 wt % methanol feed (Figure 6A), whereas the water partial pressure is considerably higher. The linear-bonded CO band was observed at 1980 cm^{-1} in completely vaporized 0.9 wt % methanol feed (spectrum a), as compared to the frequency of 1986 cm^{-1} observed at the lower system pressure of 1.36 bar. The CO band then shifted to 2020 cm^{-1} and increased in intensity when the catalyst layer was subsequently exposed to 1000 ppm CO/H_2 at 303 K and 3.08 bar (spectrum b). The lower frequency of 2020 cm^{-1} observed for the CO(L) band in spectrum b is most likely due to the higher hydrogen pressure at the high system pressure of 3.08 bar, as compared to the frequency of 2032 cm^{-1} observed in 1000 ppm CO/H_2 at 303 K and 1.36 bar. The ratio of integrated intensity of the CO(L) band in spectrum a to that in spectrum b is 0.40, as compared to the corresponding ratio of 0.55 observed at the lower system pressure of 1.36 bar. This result suggests that an increase in water partial pressure in vapor phase at 423 K at constant methanol partial pressure leads to a decrease in surface CO coverage.

Figure 7A and B shows the results of in situ ATR-IR studies of liquid-phase methanol reforming at 5.84 bar using 2 and 5 wt % methanol feed, respectively. Spectra a, b, and c in Figure 7A were collected over the time periods of 0−20, 20−40, and 40−60 min after the Pt/Al_2O_3 catalyst layer was exposed to the 2 wt % methanol feed in liquid phase at 423 K. In these three spectra, the intensity of the CO(L) band decreased with respect to the time elapsed as the catalyst layer was exposed to the liquid feed. Nevertheless, the CO(L) bands were at the same frequency of 1986 cm^{-1}. Therefore, the decrease in intensity of the CO(L) band is unlikely due to a decrease in CO coverage and is mostly likely due to a change in the catalyst film morphology (we note that the majority of the catalyst film did not detach from the ATR crystal), which decreases the amount of catalyst probed by the evanescent wave generated at the interface between the ZnSe crystal and the wet catalyst layer. To estimate the surface coverage of CO in 2 wt % aqueous methanol solution at 423 K, the catalyst layer needs to be exposed to a gas mixture containing CO to saturate the surface. As we have shown in the ATR-IR studies of WGS reaction, a change in gas atmosphere in the presence of liquid water at 373 K could lead to a change in the CO(L) band intensity. To minimize these possible artifacts, the catalyst layer was dried rapidly (<1 min) in flowing H_2 and cooled to 303 K, and it was then saturated with CO by exposing to 1000 ppm CO/H_2. Spectrum d in Figure 7A was collected after the CO-saturated catalyst layer was exposed to liquid water again. The ratio of integrated intensity of the CO(L) band in spectrum c to that in spectrum d is 0.29.

Spectra a−d in Figure 7B were collected under conditions similar to the spectra in Figure 7A, except that the methanol feed concentration was increased to 5 wt %. The linear-bonded CO band is observed at the frequency of 1990 cm^{-1}, as compared to the frequency of 1986 cm^{-1} observed in 2 wt % methanol feed, and the intensity of this band also decreased with respect to the time elapsed as the catalyst layer was exposed to the liquid feed. The ratio of integrated intensity of the CO-

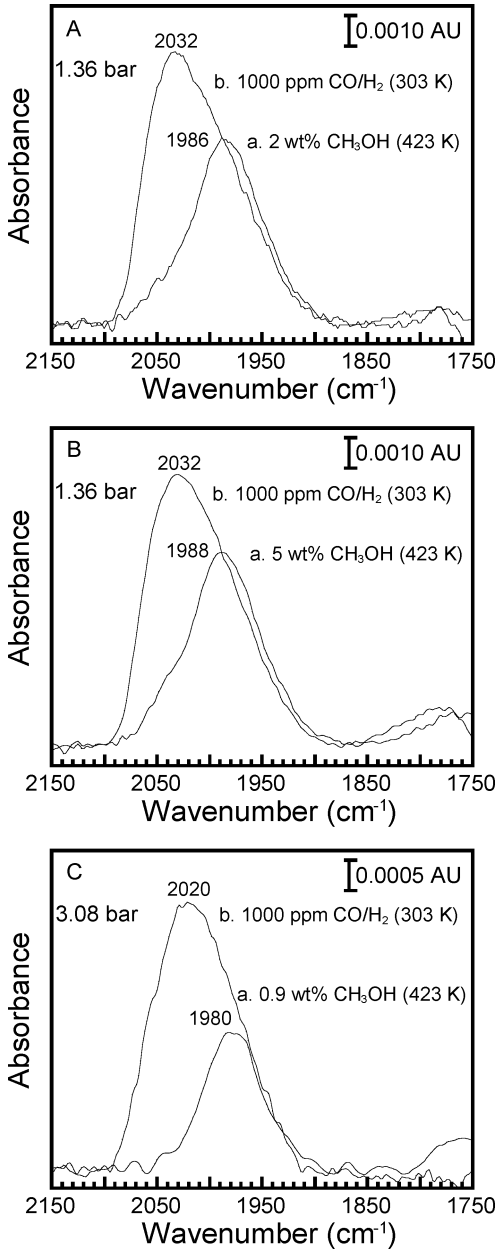

Figure 6. (A) ATR-IR spectra of CO (a) formed on Pt/Al_2O_3 as the catalyst was exposed to completely vaporized 2 wt % methanol feed at 423 K and (b) adsorbed on Pt/Al_2O_3 as the catalyst was then exposed to 1000 ppm CO/H_2 at 303 K at 1.36 bar; (B) ATR-IR spectra of CO (a) formed on Pt/Al_2O_3 as the catalyst was exposed to completely vaporized 5 wt % methanol feed at 423 K and (b) adsorbed on Pt/Al_2O_3 as the catalyst was then exposed to 1000 ppm CO/H_2 at 303 K at 1.36 bar; and (C) ATR-IR spectra of CO (a) formed on Pt/Al_2O_3 as the catalyst was then exposed to completely vaporized 0.9 wt % methanol feed at 423 K and (b) adsorbed on Pt/Al_2O_3 as the catalyst was exposed to 1000 ppm CO/H_2 at 303 K at 3.08 bar.

(L) band in spectrum c to that in spectrum d (collected for a CO-saturated catalyst in liquid water) is 0.40.

Discussion

Water−Gas Shift Reaction. Results of reaction kinetics studies of the vapor-phase WGS reaction at 373 K show that H_2 has an inhibiting effect on the reaction rate; that is, the reaction order with respect to hydrogen is −0.22. In situ ATR-IR studies carried out under conditions similar to reaction kinetics studies (with 0.4 bar H_2O at 373 K) suggest the surface CO coverages in 1000 ppm CO/H_2 and CO/He are both close

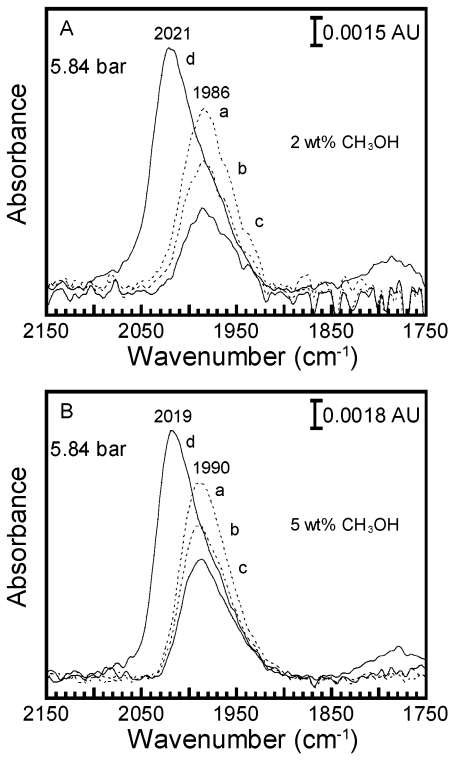

Figure 7. (A) ATR-IR spectra of CO formed on Pt/Al_2O_3 as the catalyst was exposed to 2 wt % aqueous methanol feed solution at 423 K over the periods of (a) 0−20, (b) 20−40, and (c) 40−60 min, and of CO (d) adsorbed on Pt/Al_2O_3 as the catalyst was then exposed to 1000 ppm CO/H_2 and liquid water at 303 K at 5.84 bar; and (B) ATR-IR spectra of CO formed on Pt/Al_2O_3 as the catalyst was exposed to 5 wt % aqueous methanol feed solution at 423 K over the periods of (a) 0−20, (b) 20−40, and (c) 40−60 min, and of CO (d) adsorbed on Pt/Al_2O_3 as the catalyst was then exposed to 1000 ppm CO/H_2 and liquid water at 303 K at 5.84 bar.

to the saturation coverage (∼90%). Importantly, the CO(L) band observed in 1000 ppm CO/H_2 is at a frequency of 2014 cm^{-1}, which is 8 cm^{-1} lower than the CO(L) band observed in the absence of co-feeding H_2 (in 1000 ppm CO/He). Previous studies have shown that coadsorbing H_2 with CO on Pt can lead to a small decrease of CO stretching frequency by 5−10 cm^{-1}.[42,43] Therefore, the lower frequency of CO(L) observed in the presence of H_2 gas suggests that the Pt surface has a higher coverage by adsorbed H atoms. A kinetically significant step of the WGS reaction on Pt is the dissociation of H_2O to give adsorbed OH and H species, and the reaction proceeds subsequently by reaction of OH species with CO, based on predictions from DFT calculations.[20] An increase in the surface coverage by H atoms is unfavorable for H_2O dissociation on Pt, because H atoms can block surface sites for water dissociation and H atoms can combine with OH species to convert these species back to water. Both of these effects would lead to a decrease in the rate of the WGS reaction.

Results of reaction kinetics studies of the vapor-phase WGS reaction at 373 K show that the CO partial pressure has a negligible effect on reaction rate in the presence of 1.2 bar H_2. In situ ATR-IR studies carried out using 333 and 1000 ppm CO/H_2 (with 0.4 bar H_2O at 373 K) show that the intensity of the CO(L) band increases slightly with an increase in CO concentration, and the surface CO coverage is close to saturation in both CO gas mixtures. Increasing CO partial pressure on a Pt surface with high CO coverage leads to a more poisoned surface, and hence to a lower reaction rate in the presence of 1.2 bar H_2. A negative order with respect to CO equal to −0.21

has been reported on Pt/Al_2O_3 at 543 K.[37] On the other hand, as the surface coverage by CO becomes high (at the low temperatures of the present study), then increasing the CO pressure has a small effect on the CO coverage because the differential heat of CO adsorption becomes a strong function of coverage. Therefore, the negligible effect of CO on the reaction rate observed in 1.2 bar H_2 can be attributed to the fact that the Pt surface has become essentially saturated with adsorbed CO at a gas-phase concentration of 333 ppm.

The rate of the WGS reaction in vapor phase is fractional order (0.55) with respect to H_2O partial pressure. The positive effect of H_2O can be attributed to increased OH coverage through dissociation of H_2O. A fractional order is typically observed for a reactant when the surface coverage of the adsorbed reactant becomes high, which is not consistent with the fact that adsorption of H_2O on Pt is weak.[46] Results from DFT calculations predict that the dissociation of H_2O on Pt(111) has a high activation energy barrier of 142 kJ/mol, and the subsequent step involving reaction between CO and OH species has a lower activation energy barrier of 86 kJ/mol.[47] Accordingly, the activation energy barrier for reaction of OH species with adsorbed CO is similar to the barrier for reaction of OH with adsorbed H atoms (89 kJ/mol);[47] therefore, the H_2O dissociation step may not be quasi-equilibrated. Consequently, the surface OH coverage may not be directly proportional to the surface coverage of H_2O, which is directly proportional to the partial pressure due to the weak adsorption of H_2O on Pt. Thus, the nonlinear relation between H_2O partial pressure and surface OH coverage may lead to the fractional reaction order with respect to H_2O.

In the presence of liquid water, in situ ATR-IR studies of the WGS reaction on the Pt/Al_2O_3 catalyst at 373 K show that the Pt surface is still dominated by adsorbed CO in 333 and 1000 ppm CO in either H_2 or He, based on the ratios of integrated intensities of CO bands observed at 373 K to those of CO bands observed in 1000 ppm CO at 303 K, that is, about 0.8. We note that the corresponding ratios in vapor-phase ATR-IR studies are about 0.9, which suggests that the presence of liquid water may decrease slightly the surface CO coverage under the current WGS reaction conditions at 373 K. The lower CO coverage for WGS reaction in the presence of liquid water could be due to a slightly weaker binding of CO to the Pt surface caused by displacement from the surface of weakly adsorbed water molecules. In addition, the lower CO coverage for WGS reaction in the presence of liquid water could be attributed to the presence of other adsorbed species, which are able to compete with CO for adsorption sites at high CO coverage. Results from DFT calculations suggest that the presence of liquid water may decrease the activation energy barrier of H_2O dissociation on Pt(111) from 142 to 75 kJ/mol.[47] Furthermore, the corresponding barrier could be even lower on low coordination Pt sites, which are predominant on our catalyst based on the low frequency of CO adsorbed under dry conditions. Therefore, the lower coverage of CO observed in the presence of liquid water could be caused by a higher coverage of OH species. Importantly, based on the above arguments, it appears that the rate of the WGS reaction in the presence of liquid water is comparable to the rate under complete vaporization conditions when other factors (such as partial pressure of CO) are kept constant. The rate of WGS reaction at 423 K with 2.5 mbar of CO in vapor phase was found to be 0.38 min^{-1} when only 37% of the water feed was vaporized, which is comparable to the value of 0.36 min^{-1} measured when the water feed was completely vaporized.

Methanol Reforming. The low order (0.2) with respect to methanol partial pressure observed for vapor-phase methanol reforming at 423 K cannot be attributed to a high methanol coverage on the Pt surface under reaction conditions, because methanol adsorbs weakly on Pt.[18] In situ ATR-IR studies carried out under similar conditions at 1.36 bar and 423 K show that the surface coverage by adsorbed CO increases from ~55% to ~60% of the saturation coverage as the methanol feed concentration is increased from 2 to 5 wt %. This observation suggests the Pt surface becomes more poisoned with CO as the methanol partial pressure increases in vapor phase. Therefore, the positive effect of methanol partial pressure on reaction rate is reduced by a decrease in the number of vacant sites available for methanol to adsorb and decompose, which leads to the apparent order of 0.2 with respect to methanol partial pressure in vapor phase.

The above interpretation is also supported by reaction kinetics measurements and microkinetic modeling carried out for the decomposition of methanol on Pt/SiO_2 at 473 K.[48] The reaction order with respect to methanol partial pressure was determined to be 0.16 by reaction kinetics measurements. In agreement with this result, microkinetic modeling predicts that the order is equal to 0.28 with respect to methanol partial pressure as the methanol concentration is increased from 1 to 10 wt %, which is mainly due to a decrease in the number of vacant sites as the result of an increase in the CO surface coverage.

The low order (0.3) with respect to system pressure observed for vapor-phase methanol reforming can be attributed to the effect of increasing methanol, water, and hydrogen partial pressures inside the reactor for vapor-phase methanol reforming, as shown in Table 2. We have shown that methanol partial pressure has a positive effect on the rate of hydrogen production. Reaction kinetics measurements of the WGS reaction in vapor phase at 373 K show that water partial pressure has a positive effect on the WGS reaction rate. In this respect, results of in-situ ATR-IR studies at 1.36 and 3.08 bar in completely vaporized methanol feeds show that the surface coverage by adsorbed CO decreases from 55% to 40% of the saturation coverage as the H_2O partial pressure increases (at constant methanol partial pressure). This observation suggests that an increase in H_2O partial pressure leads to higher rate of CO removal from Pt surface via the WGS reaction. Adsorbed H atoms can have a negative effect on the rate of methanol decomposition by blocking surface sites that are not poisoned with CO. Reaction kinetics measurements of the WGS reaction in vapor phase at 373 K show that hydrogen has an inhibiting effect on the WGS reaction rate. Therefore, the positive effects of methanol and water partial pressures on the rate of hydrogen production from vapor-phase methanol reforming are reduced by the negative effect of hydrogen partial pressure, which leads to the apparent order of 0.3 with respect to system pressure.

In contrast to the low order with respect to system pressure observed in vapor-phase methanol reforming, reaction kinetics measurements of liquid-phase methanol reforming show that system pressure has a strong inhibiting effect on the rate of hydrogen production. An increase in system pressure leads to an increase in hydrogen partial pressure inside the gas bubbles, which most likely inhibits methanol reforming in liquid phase by blocking surface sites with adsorbed hydrogen atoms.

The rate of hydrogen production from vapor-phase methanol reforming at 4.46 bar is much higher than that from liquid-phase methanol reforming at 4.88 bar (0.23 versus 0.08 min^{-1}). The inhibiting effect of hydrogen observed for liquid-phase methanol reforming cannot account for this observation, because

the hydrogen partial pressures are similar between the two conditions (0.05 versus 0.03 bar, respectively). The rate of the WGS reaction at 423 K in the presence of liquid water is comparable to when the water is just fully vaporized, as shown in the WGS reaction part of this discussion. Importantly, results from in situ ATR-IR studies of methanol reforming show that the surface coverage by adsorbed CO in 2 wt % aqueous methanol solution is only ∼29% of the saturation coverage, as compared to the value of 55% observed in completely vaporized 2 wt % methanol feed, which suggests that the methanol decomposition step is more kinetically limiting in liquid phase than in vapor phase. The difference of ∼3 times between the reaction rate in vapor phase and in liquid phase at 423 K corresponds to an increase of only ∼4 kJ/mol in the activation energy barrier that is involved in the rate-limiting step of methanol decomposition. The decomposition of methanol on Pt(111) is predicted to occur mainly through a pathway involving initial C−H bond activation by DFT calculations, and the highest activation energy barrier for this pathway is the initial C−H bond activation (65 kJ/mol) leading to CH_2OH species.[18−20] Under liquid-phase reaction conditions for methanol decomposition, the methanol molecules are present in hydrogen-bonded clusters with water molecules,[49,50] and the surface Pt sites that would be vacant in vapor phase are in contact with physisorbed water molecules present in the liquid phase. These differences from vapor-phase conditions could increase the activation energy barrier for the initial C−H bond activation, leading to a lower rate of methanol decomposition in the liquid phase.

Results from reaction kinetics measurements of liquid-phase methanol reforming at 423 K show that the rate of hydrogen production is near first order with respect to methanol concentration as the feed concentration increases from 2 to 5 wt %, as compared to the corresponding low order of 0.2 observed in vapor-phase methanol reforming. In situ ATR-IR studies of liquid-phase methanol reforming show that the surface CO coverage is only ∼29% of the saturation coverage in 2 wt % aqueous methanol feed, and the coverage increases to ∼40% of the saturation coverage as the methanol feed concentration is increased to 5 wt %. The corresponding CO coverages in completely vaporized 2 and 5 wt % methanol feed are 55% and 60% of saturation coverage (at 1.36 bar), respectively. These observations suggest that the Pt surface is less significantly covered by adsorbed CO for liquid-phase methanol reforming, leading to a higher reaction order with respect to methanol concentration for the reforming of methanol in liquid phase than in vapor phase.

Conclusions

Reaction kinetics studies of the WGS reaction were carried out at 373 K in vapor phase, giving reaction orders with respect to CO, H_2, and H_2O partial pressures equal to 0.02, −0.22, and 0.55, respectively. In situ ATR-IR studies carried out in vapor phase under similar conditions (in 333 and 1000 ppm CO/H_2 with 0.4 bar H_2O) suggest that the Pt surface coverage by adsorbed CO is high (∼90% of the saturation coverage) under reaction conditions. ATR-IR spectra collected in gas mixtures containing 1000 ppm CO in H_2 or He, with 0.4 bar H_2O in vapor phase, indicate that the surface coverage by adsorbed CO is similar in both gases (near the saturation coverage), and the surface coverage by adsorbed H atoms is higher in the H_2-balanced CO gas mixture. The negative reaction order with respect to H_2 partial pressure is attributed to the inhibiting effect of adsorbed H atoms on the dissociation of H_2O, which is a kinetically significant step in the WGS reaction on Pt. The positive effect of H_2O on the WGS reaction rate is most likely due to an increase in the surface coverage by adsorbed OH species. The results of DFT calculations carried out for the WGS on Pt(111), and the fractional order with respect to H_2O partial pressure, suggest that the dissociation of H_2O on Pt is not quasi-equilibrated for the WGS reaction in vapor phase.

In situ ATR-IR studies of the WGS reaction at 373 K in the presence of liquid water show that the Pt surface is still dominated by adsorbed CO in gas mixtures containing 333 and 1000 ppm CO balanced with H_2 or He; however, the surface coverage by adsorbed CO is slightly lower (∼80% of the saturation coverage) than that under complete vaporization conditions. The lower CO coverage for WGS reaction in the presence of liquid water could be due to a slightly weaker binding of CO to the Pt surface caused by displacement from the surface of weakly adsorbed water molecules, or it could be caused by a higher coverage of OH species on low coordination Pt sites as a result of faster dissociation of H_2O on the surface facilitated by liquid water. The rate of WGS reaction in the presence of liquid water is comparable to the rate under complete vaporization conditions when other factors (such as the CO partial pressure) are held constant.

Reaction kinetics studies were carried out for the reforming of methanol in vapor and liquid phase at 423 K over a total pressure range of 1.36−5.84 bar. The reaction order with respect to methanol partial pressure is 0.2 for vapor-phase methanol reforming, and it is near first order (0.7, 0.8) for liquid-phase methanol reforming. System pressure has a positive effect on the rate of hydrogen production from vapor-phase methanol reforming (order of 0.3), and it has a strong inhibiting effect on the rate of hydrogen production from liquid-phase methanol reforming. The rate of hydrogen production from vapor-phase methanol reforming at 4.46 bar is much faster than that from liquid-phase methanol reforming at 4.88 bar (0.23 versus 0.08 min^{-1}).

In situ ATR-IR studies were conducted at 423 K to estimate the surface coverage by adsorbed CO on the Pt/Al_2O_3 catalyst in completely vaporized methanol feeds and in aqueous methanol feed solutions. The surface coverages by adsorbed CO are estimated to be 55% and 60% of the saturation coverage in completely vaporized 2 and 5 wt % methanol feed at 1.36 bar, respectively. The surface coverage by CO decreased from 55% to 40% of the saturation coverage as the H_2O partial pressure increases at constant methanol partial pressure (in completely vaporized 0.9 wt % methanol feed at 3.08 bar). In contrast, the surface coverages by adsorbed CO are estimated to be 29% and 40% of the saturation coverage in 2 and 5 wt % aqueous methanol solution at 5.84 bar, respectively. To our knowledge, the present study is the first application of in situ ATR-IR spectroscopy to study a catalytic solid−liquid interface at the elevated temperature of 423 K and the pressure of 5.84 bar.

The decomposition of methanol is found to be slower during the reforming of methanol in liquid phase than in vapor phase (and hence the lower rate of hydrogen production), which could be due to a higher activation energy barrier for the initial C−H bond activation in the presence of aqueous methanol solution. The low reaction order with respect to methanol partial pressure observed for vapor-phase methanol reforming is caused by a decrease in the number of vacant sites on the Pt surface as a result of the increased extent of CO poisoning when the methanol partial pressure is increased. The surface coverage by CO during the reforming of methanol in liquid phase is lower than that in vapor phase; therefore, the number of vacant sites

on the Pt surface, available for interaction with methanol, is not as strongly affected by CO poisoning as the methanol concentration is increased in liquid phase, which leads to the near first-order reaction with respect to methanol concentration observed for liquid-phase methanol reforming. The positive effect of system pressure on the rate of hydrogen production observed for vapor-phase methanol reforming is due to the positive effects of increasing the methanol and water partial pressures, combined with the negative effect of increasing H_2 partial pressure. The inhibiting effect of system pressure on the rate of hydrogen production from liquid-phase methanol reforming is mainly caused by the negative effect of adsorbed hydrogen, which blocks the surface sites that are not poisoned by CO.

Acknowledgment. We wish to acknowledge funding from National Science Foundation (NSF), Department of Energy (DOE), and ConocoPhillips.

References and Notes

(1) Cortright, R. D.; Davda, R. R.; Dumesic, J. A. *Nature* **2002**, *418*, 964.
(2) Davda, R. R.; Shabaker, J. W.; Huber, G. W.; Cortright, R. D.; Dumesic, J. A. *Appl. Catal., B* **2003**, *43*, 13.
(3) Davda, R. R.; Dumesic, J. A. *Chem. Commun.* **2004**, 36.
(4) Shabaker, J. W.; Davda, R. R.; Huber, G. W.; Cortright, R. D.; Dumesic, J. A. *J. Catal.* **2003**, *215*, 344.
(5) Poston, P. E.; Rivera, D.; Uibel, R.; Harris, J. M. *Appl. Spectrosc.* **1998**, *52*, 1391.
(6) Dobson, K. D.; Roddick-Lanzilotta, A. D.; McQuillan, A. J. *Vib. Spectrosc.* **2000**, *24*, 287.
(7) Dobson, K. D.; McQuillan, A. J. *Spectrochim. Acta, Part A* **2000**, *56*, 557.
(8) Dobson, K. D.; McQuillan, A. J. *Spectrochim. Acta, Part A* **1999**, *55*, 1395.
(9) Zippel, E.; Breiter, M. W.; Kellner, R. *J. Chem. Soc., Faraday Trans.* **1991**, *87*, 637.
(10) Ferri, D.; Burgi, T.; Baiker, A. *J. Phys. Chem. B* **2001**, *105*, 3187.
(11) Ferri, D.; Burgi, T.; Baiker, A. *Phys. Chem. Chem. Phys.* **2002**, *4*, 2667.
(12) Ferri, D.; Burgi, T.; Baiker, A. *J. Catal.* **2002**, *210*, 160.
(13) Burgi, T.; Baiker, A. *J. Phys. Chem. B* **2002**, *106*, 10649.
(14) Ortiz-Hernandez, I.; Williams, C. T. *Langmuir* **2003**, *19*, 2956.
(15) Sexton, B. A. *Surf. Sci.* **1981**, *102*, 271.
(16) Gibson, K. D.; Dubois, L. H. *Surf. Sci.* **1990**, *233*, 59.
(17) Wang, J. H.; Masel, R. I. *Surf. Sci.* **1991**, *243*, 199.
(18) Greeley, J.; Mavrikakis, M. *J. Am. Chem. Soc.* **2002**, *124*, 7193.
(19) Greeley, J.; Mavrikakis, M. *J. Am. Chem. Soc.* **2004**, *126*, 3910.
(20) Desai, S. K.; Neurock, M.; Kourtakis, K. *J. Phys. Chem. B* **2002**, *106*, 2559.
(21) Parsons, R.; Vandernoot, T. *J. Electroanal. Chem.* **1988**, *257*, 9.
(22) Iwasita, T. *Electrochim. Acta* **2002**, *47*, 3663.
(23) Kunimatsu, K.; Kita, H. *J. Electroanal. Chem.* **1987**, *218*, 155.
(24) Chandrasekaran, K.; Wass, J. C.; Bockris, J. O. *J. Electroanal. Chem.* **1990**, *137*, 518.
(25) Beden, B.; Lamy, C.; Bewick, A.; Kunimatsu, K. *J. Electroanal. Chem.* **1981**, *121*, 343.
(26) Beden, B.; Hahn, F.; Leger, J. M.; Lamy, C.; Perdriel, C. L.; Detacconi, N. R.; Lezna, R. O.; Arvia, A. J. *J. Electroanal. Chem.* **1991**, *301*, 129.
(27) Kardash, D.; Korzeniewski, C. *Langmuir* **2000**, *16*, 8419.
(28) Beden, B.; Juanto, S.; Leger, J. M.; Lamy, C. *J. Electroanal. Chem.* **1987**, *238*, 323.
(29) Shin, J. W.; Korzeniewski, C. *J. Phys. Chem.* **1995**, *99*, 3419.
(30) Christensen, P. A.; Hamnett, A.; Munk, J.; Troughton, G. L. *J. Electroanal. Chem.* **1994**, *370*, 251.
(31) Rice, C.; Tong, Y.; Oldfield, E.; Wieckowski, A.; Hahn, F.; Gloaguen, F.; Leger, J. M.; Lamy, C. *J. Phys. Chem. B* **2000**, *104*, 5803.
(32) Park, S.; Tong, Y. T.; Wieckowski, A.; Weaver, M. J. *Langmuir* **2002**, *18*, 3233.
(33) Jusys, Z.; Behm, R. J. *J. Phys. Chem. B* **2001**, *105*, 10874.
(34) Park, S.; Xie, Y.; Weaver, M. J. *Langmuir* **2002**, *18*, 5792.
(35) Spieker, W. A.; Regalbuto, J. R. *Chem. Eng. Sci.* **2001**, *56*, 3491.
(36) Regalbuto, J. R.; Navada, A.; Shadid, S.; Bricker, M. L.; Chen, Q. *J. Catal.* **1999**, *184*, 335.
(37) Grenoble, D. C.; Estadt, M. M.; Ollis, D. F. *J. Catal.* **1981**, *67*, 90.
(38) Lam, C. W.; Stacey, M. S.; Trimm, D. L. *Chem. Eng. Sci.* **1981**, *36*, 224.
(39) deMenorval, L. C.; Chaqroune, A.; Coq, B.; Figueras, F. *J. Chem. Soc., Faraday Trans.* **1997**, *93*, 3715.
(40) Kappers, M. J.; Vandermaas, J. H. *Catal. Lett.* **1991**, *10*, 365.
(41) Greenler, R. G.; Burch, K. D.; Kretzschmar, K.; Klauser, R.; Bradshaw, A. M.; Hayden, B. E. *Surf. Sci.* **1985**, *152*, 338.
(42) Eischens, R. P. *Acc. Chem. Res.* **1972**, *5*, 74.
(43) Vannice, M. A.; Twu, C. C.; Moon, S. H. *J. Catal.* **1983**, *79*, 70.
(44) Bourane, A.; Dulaurent, O.; Bianchi, D. *Langmuir* **2001**, *17*, 5496.
(45) Primet, M.; Basset, J. M.; Mathieu, M. V.; Prettre, M. *J. Catal.* **1973**, *29*, 213.
(46) Wagner, F. T.; Moylan, T. E.; Schmieg, S. J. *Surf. Sci.* **1988**, *195*, 403.
(47) Desai, S.; Neurock, M. *Electrochim. Acta* **2003**, *48*, 3759.
(48) Gokhale, A. A.; Kandoi, S.; Greeley, J. P.; Mavrikakis, M.; Dumesic, J. A. *Chem. Eng. Sci.* **2004**, *59*, 4679.
(49) Wei, S.; Shi, Z.; Castleman, A. W. *J. Chem. Phys.* **1991**, *94*, 3268.
(50) Wakisaka, A.; Abdoul-Carime, H.; Yamamoto, Y.; Kiyozumi, Y. *J. Chem. Soc., Faraday Trans.* **1998**, *94*, 369.